HIGH SCHOOL EDITION
Journal of Student Research
Volume 11 Issue 4 (2022)

An Experimental Investigation on the Generation of Lift by a Flat Plate

Graham Wild

Lyneham High School, Australia

ABSTRACT

Background: The aviation industry is not only essential for travel around a large country such as Australia, but it is also a significant part of the economy employing many people, including pilots. With the industry's growth, there is a need to train and educate more pilots, who require a correct working knowledge of lift and flight. *Aim*: The purpose of this study was to experimentally measure the lift generated by a flat plate to demonstrate that the shape of a wing is not important to the lift produced in a low-cost repeatable manner. *Method*: A small wind tunnel was constructed, with a flat plate airfoil mounted on digital scales to measure lift and an Arduino controlling servos to alter the angle of attack in the airflow. *Results*: The measured lift slope of 0.113/deg agrees with the theoretical value of 0.109/deg. This was achieved with a total cost of less than $200 USD. *Conclusions*: The findings show that a flat plate produces as much lift as a curved airfoil, which can be readily shown in a simple homemade wind tunnel. *Recommendations*: Education and training materials in high school science and in aviation training syllabi need to be modified to correctly explain how lift is generated.

Introduction

Significance

Thornhill (2017) states that 95% of people today have been on an airplane at some point in their life. Seeing a plane flying overhead is a daily occurrence for many people. The aviation industry is so large that it is worth $2.7 trillion US (Asquith, 2020); if this were a country, it would be the 20th largest economy, equivalent to Switzerland (Asquith, 2020). Aviation provides 65.5 million jobs worldwide, including directly related jobs like pilots, flight crew and airport staff, as well as indirect jobs such as cargo, logistics, and manufacturing (Asquith, 2020). Salas (2022) explained that within the next 20 years, 130,000 new pilots will be needed in the US alone; this is roughly a quarter of what the world will need. The current theories of lift that are taught to pilots are incorrect (McLean 2012, McLean 2018a, McLean 2018b). A correct understanding of aerodynamics is essential for pilots in situations like the infamous Air France 447 accident (Palmer, 2013).

Background

Pressure is the force a fluid exerts perpendicular to an area (Kermode, 2013). Pressure arises due to the motion of molecules of the fluid impacting the surface of a solid object.

Equation 1: Pressure (P) relation to force (F) and area (A) (Kermode, 2013):

$$P = \frac{F}{A}$$

Pressure is measured in Newtons per square meter, referred to as Pascals (Pa). At sea level, the average surface pressure is 101,325 Pa; this is approximately equal to 10,000 kg pressing down on every square meter of the earth's surface (Kermode, 2013).

Density is the mass of a substance per cubic meter (Kermode, 2013).

Equation 2: Density (ρ) relation to mass (m) and volume (V) (Kermode, 2013):

$$\rho = \frac{m}{V}$$

For water, this has a value of 1,000 kg/m^3 and for air is 1.225 kg/m^3. Therefore, a liter of air is almost 1,000 times lighter than a liter of water.

Pressure and density in a liquid are related.

Equation 3: Pressure density relation (Kermode, 2013):

$$P(h) = \rho g h$$

Here h is the height/depth of the liquid and g is the local acceleration due to gravity, or 9.796 m/s^2 for Canberra, Australia (Adams, 2014). This is the principle of a u-tube manometer (Popoola, 2017). A manometer is an instrument used to measure pressure. An example is illustrated in Figure 1, where a difference in pressure results in a difference in height in the two sides of the "u" shaped tube.

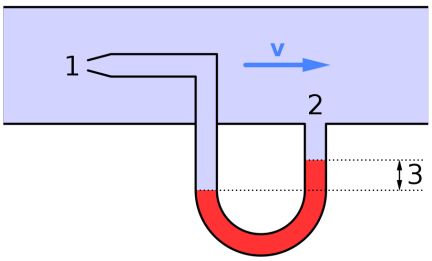

Figure 1. Pitot Tube and a u-tube manometer to measure airspeed in a tunnel (MikeRun, 2019). The total pressure acts at 1 while only the static pressure acts at 2, and the difference between them is the dynamic pressure illustrated as 3.

The relationship between pressure and density in a gas is captured in Bernoulli's equation (Kermode, 2013). Bernoulli's equation is only applicable to incompressible fluids, where density is constant. Bernoulli's equation does not apply to regions where viscosity is important. Viscosity is a measure of intermolecular attraction in a fluid and is related to the stickiness of a fluid.

Equation 4: Bernoulli's equation (Kermode, 2013):

$$P(T) = P + 0.5\rho v^2 + \rho g h$$

Here P(T) is the total pressure and is given as the sum of the static pressure (P), the dynamic pressure ($q = 0.5\rho v^2$), and the height or head pressure, P(h). This concept is illustrated in Figure 1, where the total pressure (the sum of the static and dynamic pressure) acts at the perpendicular orifice of the Pitot tube (location 1), and only the static pressure acts on the parallel orifice, called the static port (location 2). Ignoring the

height/head pressure term, the difference between the total pressure and the static pressure is the dynamic pressure (Kermode, 2013). Assuming a constant density, the dynamic pressure is then a measure of the flow velocity.

When a plane flies, the wing goes through the air; as the wing makes contact with the air flowing towards it, the air stagnates (Kermode, 2013). This occurs at the end of the streamline that divides the flow into the portion induced up over the wing, and the portion that flows underneath. Between these, there must be a point that neither goes over or under; as such, the air stops perpendicular to the surface, losing all speed. As such, the stagnation point is a high-pressure region near the leading edge of the wing; this results in a pressure gradient force (PGF) that accelerates the air above and below the wing (Mclean, 2012). The PGF is the force responsible for wind blowing from regions of high surface pressure to low surface pressure. The air that goes beneath the wing is accelerated less by the weaker PGF in that direction, producing a relatively higher pressure below. Conversely, the air above the wing is accelerated more by the stronger PGF; this produces a relatively lower pressure above. This difference in pressure between the upper and lower surface is what aerodynamicists measure to determine lift (Wild, 2021). Because the air is faster over the top relative to the air underneath, the flow appears to circulate around the wing; circulation can be used to calculate how much lift is generated (Wild, 2021). There is one more important feature of the flow around a wing in terms of lift; the flow must turn downwards, which in 3D flow is referred to as downwash (Kermode, 2013). All these features of the flow are explained by Navier-Stokes, which importantly includes viscosity which is essential to produce the asymmetric flow that occurs around a wing (Liu, et al., 2017). Figure 2 shows the airflow around a wing cross-section or an airfoil.

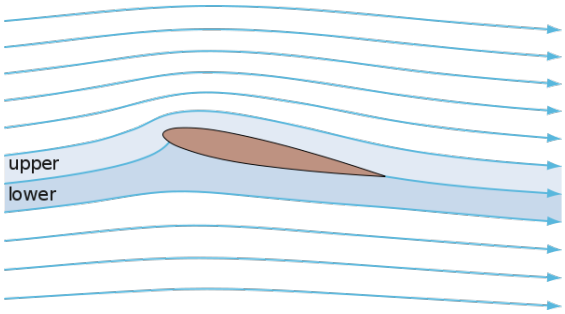

Figure 2. The airflow around an airfoil showing the flow above and below, and the stagnated streamline between them, where the initial high-pressure region is located at the surface (Belisle, 2008).

If an aircraft is flying at a constant altitude at a fixed speed, then the force of lift must balance the weight. This is Newton's 3rd Law. We can then use Newton's 2nd Law to give the weight, and hence lift.

Equation 5: Newton's 2nd Law for a weight force (W) (Kermode, 2013):

$$W = mg$$

Here m is the mass in kilograms. The lift force is provided by fundamental aerodynamics (Kermode, 2013).

Equation 6a: The lift force (L) using q (Kermode, 2013):

$$L = C_L qS$$

or

Equation 6b: The lift force (L) substituting in the definition of q (Kermode, 2013):

$$L = C_L 0.5\rho v^2 S$$

Here C_L is the coefficient of lift, and S is the surface area of the wing. As previously indicated, the dynamic pressure (q) can be measured by the u-tube manometer. According to thin airfoil theory, the coefficient of lift for a symmetric airfoil only depends on the the angle of attack ($\boldsymbol{\alpha}$) (Kermode, 2013).

Equation 7: Thin airfoil theory coefficient of lift for a symmetric airfoil ($\boldsymbol{\alpha}$ in degrees):

$$C_L = 0.109\alpha$$

Figure 3 shows the angle of attack.

Figure 3. The geometry of an airfoil showing the angle of attack between the chord line and flow direction (Mclean, 2014).

There are several homemade wind tunnels demonstrated on YouTube. Markwaller99 (2018) shows how a wind tunnel can be made with the air being sucked in, depicted in Figure 4 (top left). Ericinventor (2014) created a wind tunnel with an almost completely different design with the fan blowing air into a cylindrical pipe attached to a plexiglass box containing part of a plane wing model with the ability to rise when the tunnel is on, Figure 4 (middle bottom). Goel (2015) built a wind tunnel that blows air into the tunnel like most; this is slightly different to sucking air in, Figure 4 (top right). If the air is blown, it spirals more than if it is sucked in, which is a problem as you would not be able to see the smoke/steam flowing straight through the tunnel. The air can be straightened by using a flow straightener that can be made using lots of long tubes or straws. The wind tunnels that blow air in need smaller straighteners (straws) to straighten the larger spirals, whereas sucking air in requires less flow straightening. Other similar work (Damon Dallas 2018; Michael Dean Funston 2020) state how the wind tunnel can be made. While most use different ways of fabricating a wind tunnel, they all work in a similar way and can achieve similar results. Of the five examples, three had the test section after the fan (blowing) and two had the test section after the fan (sucking). Only two of the five measured the airspeed, both with an anemometer. Two used steam/fog to visualize the flow and three tested wings/airfoils. While previously discussed, homemade wind tunnels focused on smoke flow visualization measuring a force is common in experimental aerodynamics (Kermode, 2013). Using a digital scale and a simple wind tunnel has been demonstrated by Weltner (1990) and others (Oss, et al., 2010). A simple way to measure pressure in a wind tunnel is with a u-tube manometer (Liang & Wei, 2018). Another interesting way to measure air pressure in a simple wind tunnel was demonstrated by Macchia and Vieyra (2017), who used the barometric sensor of a smartphone.

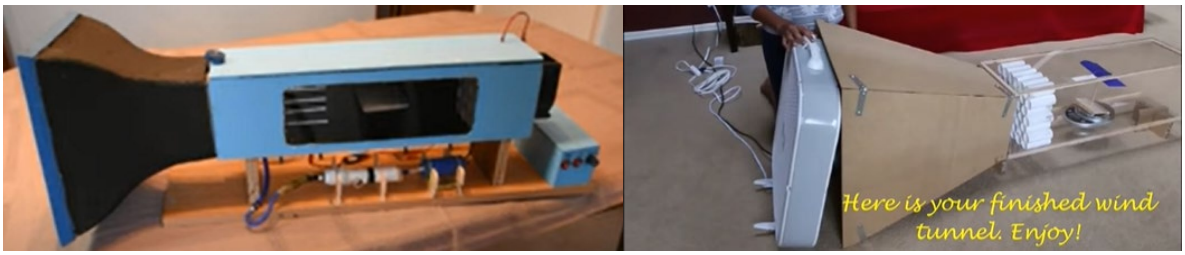

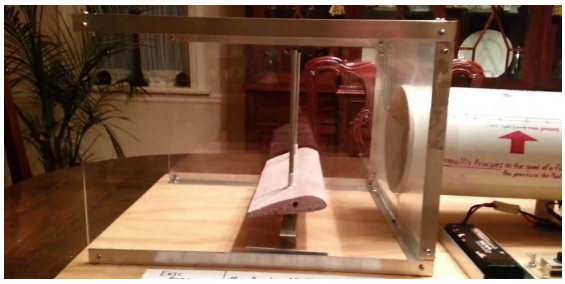

Figure 4. Images from a sample of wind tunnel project videos posted on YouTube.

Aim

This work aimed to show that lift is not only produced by a curved wing and that a flat plate produces the same amount of lift. That is, the aim is to show that a curved wing is not special in terms of lift production. Furthermore, the relationship between lift and angle of attack are quantified. To achieve these objectives, the experiment involved the construction of a wind tunnel. A u-tube manometer was created to measure the airspeed inside the wind tunnel with a Pitot tube and applying Equation 3 and Equation 4. A box fan was used to suck air through the wind tunnel, given that previous wind tunnels investigated showed better flow properties, relative to blow through wind tunnels. The angle of attack between the airfoil and the airflow was varied to produce a range of lift forces. Using Equation 5 and Equation 6, the relationship in Equation 7 was plotted. This was then compared to theoretical data for a NACA 0012 symmetric curved airfoil (Sheldahl, & Klimas, 1981).

Hypothesis

It was hypothesized that the flat plate would produce the same lift as the normal curved wing at low angles of attack. Also, the flat plate would produce less lift at higher angles of attack, as the airflow stalls and separates from the upper surface (Kermode, 2013). The next hypothesis was that the lift would increase as a function of the angle of attack prior to stall (Kermode, 2013). The final hypothesis was that the u-tube manometer would be accurate enough to tell the difference between the three airspeeds, given that they are commonly used (Liang & Wei, 2018).

Methods

Equipment

To complete this project, several items needed to be acquired (many of them were items already available from craft and home renovation projects). In addition, a few common power tools were required to complete the fabrication. A complete list is given here:

- Wind tunnel structure
    - Plywood, 6mm sheet
    - Pine wood
    - Timber screws
    - Acrylic sheet, 3mm
    - Adjustable kitchen cabinet legs, plastic
    - Split hinges
    - Latches

    - Weather sealing strip
    - Duct tape
    - 20mm PVC conduit
    - Bamboo skewers
- 38cm Box fan
- Test and measurement
    - 6mm metal rod
    - RC push rod and ball joints
    - Blue Foam
    - Digital high precision scale
    - Arduino uno kit
        - Bread board
        - Jumper wire
        - Potentiometer
    - Servos
    - Laptop
- Glue/adhesives
    - Hot glue
    - Spray adhesive
    - General purpose adhesive
    - Construction adhesive
- Power tools
    - Drill and bits
    - Driver and bits
    - Renovator (sanding and trimming)
    - Circular saw

Setup

Figure 5 shows the dimensions of the wind tunnel as planned. Figure 6 shows a photo of the final constructed wind tunnel. The details needed for the Arduino servo control were taken from the official documentation (Arduino, 2022).

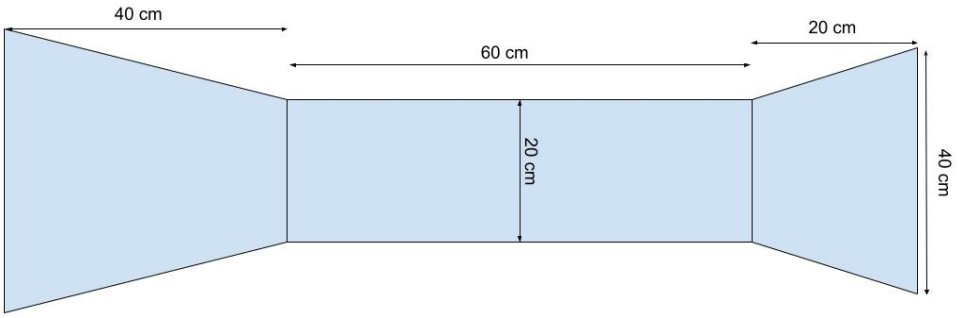

Figure 5. Dimensions of the wind tunnel.

Figure 6. Final constructed wind tunnel with digital scales and box fan.

Procedure

Initially, a quarter scale (1 inch = 10cm) was constructed from cardboard. In this, four rectangular pieces were used to make a square-based prism for the tunnel test section. Two truncated square-based pyramids were used as the inlet and outlet, with the outlet being twice the length of the inlet. These were constructed from 4 trapezoids each. Basic trigonometry was used to give the required perpendicular heights. This ensured that all of the pieces fit together correctly.

Constructing the wind tunnel involved cutting the plywood to match the scaled-up cardboard pieces from the model. In total, 11 pieces were needed, with one rectangle replaced by an equivalent-sized piece of acrylic. This was used to see the angle of the wing on the inside and to facilitate future flow visualization.

The framing for the test section was constructed with eight pieces of 42mm by 30mm pine, trimmed with the 20cm internal length, with 45-degree end cuts. The framing for the inlet and outlet used 42mm by 19mm pine. Trigonometry was used to determine the bevel angle, which was cut using a handheld circular saw. Again, the internal edges were 20cm with 45-degree end cuts and the bevel on the correct side.

Overall, the structure had a semi-monocoque design. That is, the frame was used to maintain the shape of each piece that were joined to maintain the structure of the wind tunnel. The frames were screwed together externally, and countersunk screws were used internally to attach the panels. Glue and sealant were used on all the joins to make it airtight. Next, the inlet and outlet were attached to the test section using split hinges on the top, and latches on the bottom. This was done to enable the tunnel to be easily transportable. Finally, cabinetry legs were attached to the bottom of the wind tunnel to give space below for scales. To complete the tunnel, holes were drilled in the bottom of the test section for the mounting, and the fan was attached to the outlet side of the wind tunnel, drawing in air through the tunnel. The gap between the fan and the tunnel was sealed with duct tape.

The airfoil was made from a 3mm thick piece of plywood that was 10cm in chord. The length was continuously trimmed such that it fit inside the tunnel test section without it rubbing on the walls. The length and width of the airfoil were recorded to give the surface area. General radio-controlled components were used to enable the angle of attack to be changed. The socket end for a push-rod ball connector was glued into the airfoil a quarter of the way from the front (at the aerodynamic center). The corresponding ball connector was adhered to the end of the 6mm steel rod. The length of the metal rod was estimated with the legs on the wind tunnel, the height of the scales, and the noting where the airfoil would sit in the test section. The other end of the rod was held in a piece of pine that was adhered to the scales. Also attached towards the rear of the piece of pine were two lengths of plywood to house a servo each. The servos were attached to the rear of the airfoil via two ball link connectors at the same distance from each side of the airfoil. The servos were connected to an Arduino Uno which was controlled via a laptop. The input to control the angle of attack was a potentiometer, with code written to control the mechanisms.

Measuring the dynamic pressure required the fabrication of a u-tube manometer. This utilized a long length of clear hose with a ruler to measure the height change of the water inside. Inside the wind tunnel, the

hose was connected to drinking straws to act as a pitot tube like Figure 1. At one end, a bendy straw was directed into the airflow, while at the other end, the straw was normal to the airflow. With the pitot tube in the wind tunnel, four measurements were taken, corresponding to the fan's four settings: off, low, medium, and high. For each measurement, a photo of the u-tube manometer was taken for analysis. These images were uploaded to Google Slides, where the heights of the meniscus in each side of the manometer could be accurately measured, well beyond the resolution of the millimeter scale rule used. The speed calculation involved the difference in the height of the menisci, in Google Slide centimeters. To enable this, a line was drawn "horizontal" from the bottom of each meniscus to the edge of the rule with the mm markings. Next, a line perpendicular to these was created with a copy, paste, and rotate in Google Slides. The length of this line was reduced to the size of the gap between the two horizontal lines. Next, a line that was 5mm in length was drawn along the edge of the rule. The length of this as an object in Google Slides relative to 5mm gives a scaling factor to convert the Google cm into real mm. Noting the acceleration due to gravity and density of water, the pressure could be determined using Equation 3.

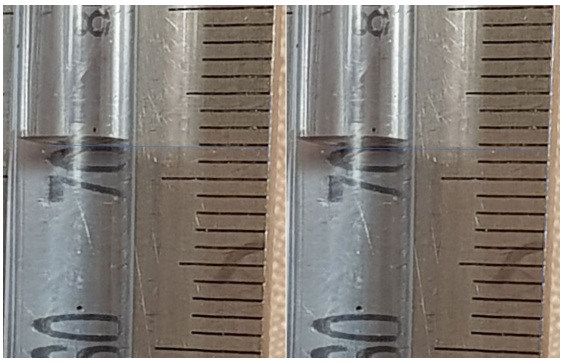

Figure 7. Photos of water level in the u-tube manometer, without airflow on (left) with (right). The blue lines indicate the level at the bottom of the meniscus.

Next, the flat plate airfoil was placed in the wind tunnel and measurements were taken at different angles. The measurements included recording the mass of the flat plate within the wind tunnel and taking a photo of the plate to calculate the angle accurately. This was done relative to a digital inclinometer (level) placed on top of the tunnel test section. The angle between the vertical (horizontal) and the wind tunnel was measured with the inclinometer, and then in the images, the angle between the wind tunnel and flat plate was determined. These angles combined give the angle of attack. This was done for 10 angles and only at the fastest speed setting. For the mass measurements, given the highly variable nature of flow, 20-second videos were captured of the change in the weight for each angle. Watching the videos resulted in recording the highest and lowest values, which were then used to give an average mass. This average was calculated in Google Sheets.

The angle measurements of the plate in the tunnel involved importing the images into Google Slides to undertake a similar analysis as for the u-tube manometer. First, a line was drawn along the bottom edge of the wind tunnel as a reference line. This was copied and moved to intersect the trailing edge of the plate in the image. This became the adjacent side of the triangle (similar to Figure 3). This line was copied and rotated 90 degrees, then moved and shortened to become the opposite side. A hypotenuse of the triangle was then created from the trailing edge to the leading edge. From the object properties in Google Slides, the horizontal and vertical dimensions were taken for each of the 3 lines. These dimensions were placed into Google Sheets.

The Google Sheet at this stage contained information about the speed calculation, the masses, and the angle of attack. The two mass measurements (max and min) were averaged in another column. Next, the zero-flow mass reading was subtracted, and the result was converted to weight using Equation 5. For the angles, the three pairs of dimensions for the lines were converted into lengths using Pythagoras. These three lengths were then used with the three trig identities (sin, cos, and tan) to give 3 estimates of the angle, which were averaged

in another column. The angle correction from the inclinometer was applied. Next, the weight was divided by the dynamic pressure and the area to give the coefficient of lift for each of the measurements. Finally, the angle of attack versus the coefficient of lift can be plotted. Noting where the stall occurs, a second plot can be created without the stall, such that only the linear part of the data is used. To this, a line of best fit with the equation to give the lift slope can be added.

Figure 8. Screen shot from recording of digital scale reading with zero-flow.

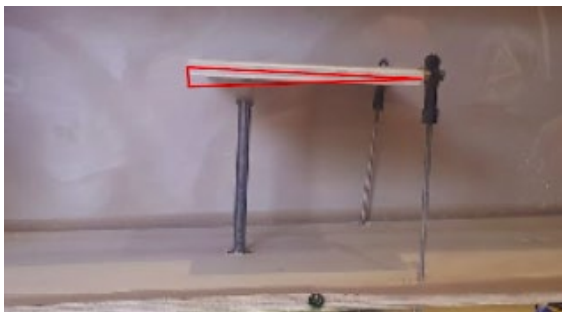

Figure 9. Example image of airfoil in the wind tunnel, with added triangle used to determine the angle of attack.

Results

Dynamic Pressure

Figure 7 shows the height change within the u-tube manometer. Using the image and Pythagoras, the change in height in mm was determined. A line 5mm long was drawn along the rule, and this had a height of 3.02cm and a width of 0.11cm in the Google Slide. This corresponds to a conversion of 5/3.022 mm/cm. The height of the first meniscus was 11.08cm, and the second was 10.96cm giving a difference of 0.12cm. This then converts to 0.1985mm. Using equation (3) the dynamic pressure can then be determined assuming g = 9.796 m/s^2 and the density of water is 1000kg/m3. This gives a pressure of 1.95Pa. Table 1 includes all the relevant parameters.

Table 1. Relevant parameters for the dynamic pressure.

Parameter	value	Units
h	0.0001985	m
p	1000	kg/m^3
g	9.796	m/s^2
q	1.95	Pa
v	1.78	m/s

Angle of Attack and Lift

Table 2 shows the results from the triangles drawn in Google Slides used to determine the corresponding angles of attack. Using Pythagoras, the x and y values were converted into lengths of the corresponding sides. Then using trigonometry (sin, cos, and tan) the angle of attack for each triangle was calculated 3 ways and averaged.

Table 2. Horizontal (x) and vertical (y) components in cm from Google Slides for the angle of attack triangles, giving the resultant average angles of attack and corresponding measured lift forces.

	Opposite		**Adjacent**		**Hypote-nuse**		**AoA**	**Lift**
Trail	**x**	**y**	**x**	**y**	**x**	**y**	**deg**	**N**
1	1.13	0.03	4.74	0.12	4.75	1	14.38	0.087
2	1.22	0.07	4.04	0.33	4.1	0.89	17.52	0.076
3	1.03	0.04	3.86	0.2	3.92	0.82	16.31	0.086
4	0.07	0.75	3.3	0.25	3.36	0.49	14.16	0.086
5	0.55	0.03	3.18	0.2	3.22	0.33	11.22	0.077
6	0.03	0.46	3.02	0.14	3.05	0.32	10.29	0.076
7	0.49	0.03	3.43	0.16	3.44	0.31	8.80	0.069
8	0.01	0.39	3.45	0.16	3.49	0.23	8.61	0.059
9	0.35	0.03	3.88	0.29	3.91	0.05	6.65	0.054
10	0.27	0.01	3.15	0.1	3.15	0.16	5.33	0.035

From the 10 videos, the maximum and minimum masses were recorded and averaged. The zero-wind speed mass was subtracted (8.785g, this would alternate evenly between 8.78 and 8.79). Using Equation 5, these were converted to forces, also included in Table 2.

Lift Slope

Using equation 6, the lift force was converted to a coefficient of lift. Figure 10 shows the coefficient of lift plotted as a function of the angle of attack. Included in Figure 10 are the theoretical values for a simple symmetric airfoil, NACA 0012 (Sheldahl, & Klimas, 1981). In Figure 11, the linear portion of the data is re-plotted. With this, a line of best fit is included showing the lift slope measured in the experiment. The value is 0.113/deg. This experiment shows that lift is not only produced by a normal curved wing and that a flat plate will produce the same amount of lift.

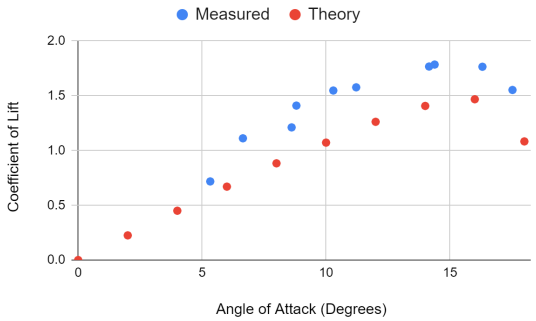

Figure 10. Coefficient of lift as a function of angle of attack measured for the flat plate compared to the theory for a thin curved airfoil.

Discussion

Findings

The lift slope for the flat plate airfoil was measured as 0.113/deg. However, the theoretical value from the thin airfoil theory is 0.109/deg (Kermode, 2013). This corresponds to a difference of 0.004, which relative to the theoretical value corresponds to a 3.7% error. The measured number is only 3.7% bigger than the theoretical number expected.

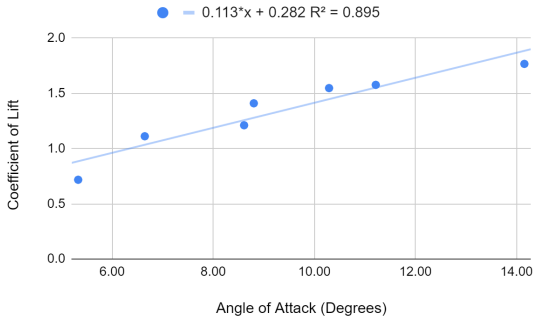

Figure 11. Lift slope determination from the line of best fit on data without stall.

Many similar experiments on YouTube exclusively use flow visualization (Waller, 2020). This is done with a humidifier or a source of smoke like a vape pen. In this work, we have demonstrated the ability to quantitatively measure lift. The reduction in lift due to stall was also observed, which is typically highlighted with flow visualization.

Importantly lift was clearly produced by a flat plate without a curved surface. As such, the curved shape of an airfoil is not responsible for producing lift; in fact, that shape results in less drag (Anderson & Eberhardt, 2010). Interestingly an explanation for lift based on the Coanda effect requires a curved surface (Anderson & Eberhardt, 2010), which is not present in this experiment. This adds to the point that Coanda is clearly not applicable when it comes to explaining lift. Further, the Coanda effect is required to be taught to pilots in Australia, as regulated by CASA.

Limitations

Using online sources, the speed of air through a household fan was expected to be 3m/s. The wind tunnel was designed with an area reduction of 4, which corresponds to a velocity increase by the same factor. Initially, we expected a wind speed of 12m/s; this would correspond to a u-tube reading of 7.2mm. Unfortunately, the measured peak speed was 1.78m/s, in the test section. The exact reason for this is unknown. However, it is clear the household fan does not work efficiently, with its rear flow significantly restricted. The flow straightener may be another serious source of flow restriction. However, without its use, the readings on the manometer were not stable.

The wind speed issue resulted in issues with dynamic pressure measurements. That is, the low speeds corresponded to sub-millimeter height changes. Unfortunately, these could not be resolved. As such, to facilitate continued experimentation, only the high-speed setting was utilized, and the planned investigation into the effect of flow speed was dropped.

Initially, it was anticipated that the angle of attack would be varied from zero to 20 degrees in 2-degree increments. However, the crude mechanism for connecting the airfoil to the scales limited controllability. As the servo was moved to higher or lower values, the push rods would push against the edge of the holes drilled

into the bottom of the wind tunnel applying an additional force that was much greater than the lift force. The result was to simply limit the movement of the servos and take readings where the push rods did not rub on the wind tunnel.

Future Work

The most significant improvement in future work would come from the use of a fan designed for purpose that can cope with the significant flow restriction. For example, a $200 AUD industrial fan would produce a wind speed of 25m/s. This would resolve the issues measuring the small dynamic pressures. However, a very sensitive pressure sensor could be used with the Arduino to measure very small pressure changes. Alternatively, a small anemometer could be used instead of a pitot tube to measure the wind speed. This needs to be small, as the housing etc. of the device will restrict airflow and hence produce a resultant artificial increase in flow speed relative to when the device is not in the flow.

Ideally, the control of the angle could be done in software by calibrating the system. To further utilize the Arduino, a load cell could be used in place of the digital scales, which just use a load cell. This would enable the angle to be set and for the lift force to be measured in software. With the use of a better fan, an Arduino compatible pitot tube could readily be used to also measure the flow speed (dynamic pressure). This would fully automate the entire system, enabling easy reproduction of results by multiple users.

With the availability of 3D printers and other homemade maker technology, constructing different test samples would also be feasible. That is, different wings with different shapes could be utilized, enabling students to replicate the early work of the Wright brothers in their wind tunnel with lots of different planforms and cross sections. Also, the effect of high lift devices could be easily investigated, making airfoils with flaps and slats etc.

Recommendations

This work demonstrates the fabrication of a simple homemade wind tunnel used to investigate the lift being generated by a flat plate. Unfortunately, the current high school science curriculum does not provide sufficient understanding about lift to explain the results presented. As such, it is recommended that the syllabus change to include a qualitative understanding of Navier-Stokes (Wild, 2021), specifically the key role of viscosity in changing the shape of the flow field around an airfoil to resolve D'Alembert's paradox.

Replication Studies

Some suggestions can be made for those who would like to replicate this study. First, the most expensive component was the 0.01g digital scales. This was used as it was readily available for a home workshop and previously used in a year 7 science project. However, the resolution shown in Table 2 suggests that a 0.1g scale would be sufficient. At 1g, the values range from 4 to 9, which could make the experiment harder, although this would be a good application of repeated trials and signal averaging to reduce the noise. The advantage of 0.1g scales is that they are readily available for $15 USD ($30 AUD from a local supplier). As mentioned in the future work section, a better fan is a worthy investment, which would also offset the need for 0.1g scales.

For some of the construction, some substitutions would also be suggested. For example, the inlet and outlet do not need to be as heavy and could be made from 3mm ply instead of 6- or 7-mm ply. This would reduce their weight. The test section, however, needs to be more rigid and hence should be made of 6- or 7-mm ply. Table A1 in the Appendix includes an indicative list of items and costs from an Australian hardware store. The only item not fairly reflected in terms of price is the acrylic sheets, which from a specialist supplier would be $10. That puts the total construction cost at $120 AUD or less than $85 USD. In addition to this, a box fan

is needed. Unfortunately, the 38cm box fan used in this project is relatively old, and hence an alternative is not readily available online. Box fans more commonly come in 12-inch and 20-inch sizes, 30 and 50 cm, respectively. For the larger size, looking at Amazon, this would be $90 AUD or in the US only $35 USD. The final requirement is an Arduino Uno kit with servos, and a typical starter kit with accessories includes one servo, with another costing dollars ($5). When sourced locally, the Arduino Uno starter kits on Amazon are currently around $50 AUD and $45 USD,.

The exact item used to mount the airfoil on the metal rod from the scale was a Dubro Threaded Ball Link 1.6mm. The threaded ball link was attached to the end of the metal rod with a small 3D printed plastic connector, epoxied together. If possible, the rod could be drilled and threaded to fit the ball link. Similar, an easier method could be to use hot glue to build up plastic on the tip of the metal rod. Next, the servos were connected to the rear of the airfoil by 2 Dubro Heavy Duty Threaded Ball Link (4-40). The balls mounted on the nuts were screwed and glued into small holes drilled into the rear of the airfoil, and the split ball connector was attached to the threaded end of the 2 push rods. The total cost of all of this was $10 ($4 for the 1.6mm ball link, $2 each for each 4-40 link and push rod). The details of this are shown in Figure A1 of the Appendix.

The total cost to replicate this work is $195 USD. However, for the work completed in this study, because of the availability of the materials, only $55 AUD, or $38 USD was needed (metal rod, 42x19 pine, legs, hinges, latches, and servo linkages). The choice to use an Arduino to control the servos was made because one was available. Similarly, the size of the wind tunnel was based on the availability of the 38cm box fan.

Conclusion

The experiment shows that lift is not only produced by a normal curved wing and that a flat plate will produce the same amount of lift. That is, a curved wing is not special in terms of lift production. The relationship between the angle of attack and lift was quantified. However, the relationship between airspeed and lift was not quantified as the desktop box fan suffered from significant flow restriction producing significantly lower flow speeds than expected. The coefficient of lift was successfully plotted as a function of the angle of attack. This was compared to theoretical data for a NACA 0012 symmetric curved airfoil. The flat plate produced promising results similar to the NACA 0012 airfoil as hypothesized. The flat plate produced a similar amount of lift as the normal curved wing at lower angles of attack (AoA). However, the flat plate lost lift sooner than the NACA 0012 symmetric curved airfoil. Although it had a minuscule change in height, the u-tube manometer when coupled with modern digital imagery, the method to measure airspeed was fairly accurate for the fastest speed tested.

Acknowledgments

I would like to thank my advisor for the valuable insight provided to me on this topic.

References

Adams, B., 2014. Local Acceleration of Gravity. Wolfram. Available at: https://www.wolframalpha.com/widgets/view.jsp?id=e856809e0d522d3153e2e7e8ec263bf2.

Anderson, D. F., & Eberhardt, S. 2010. Understanding flight. McGraw-Hill.

Arduino, 2022. Servo Motor Basics with Arduino: Arduino Documentation. Retrieved from https://docs.arduino.cc/learn/electronics/servo-motors

Asquith, J., 2020. If Aviation Was A Country It Would Be The World's 20th Largest By GDP. Forbes. Available at: https://www.forbes.com/sites/jamesasquith/2020/04/06/if-aviation-was-a-country-it-would-be-the-worlds-20th-largest-by-gdp/?sh=75c4d54ee5b5.

Belisle, M., 2008. Streamlines around a NACA 0012. Wikimedia Commons. Available at: https://commons.wikimedia.org/wiki/File:Streamlines_around_a_NACA_0012.svg.

Dallas, D., 2018. Engineering 150: Wind Tunnels. YouTube. Available at: https://www.youtube.com/watch?v=Pplbm8VJxfo.

ericinventor, 2014. Homemade Wind Tunnel. YouTube. Available at: https://www.youtube.com/watch?v=qDQncRSlL8c.

Funston, M., 2020. DIY Wind Tunnel. YouTube. Available at: https://www.youtube.com/watch?v=ROfvzjQkfOs.

Goel, A., 2015. Wind Tunnel Science Project. YouTube. Available at: https://www.youtube.com/watch?v=Dm3uNAq5aHU.

Kamal, Z., 2018. Subsonic Wind Tunnel. YouTube. Available at: https://www.youtube.com/watch?v=xXYfYPE5D8A.

Kermode, A.C., 2013. Mechanics of flight, Pearson.

Liang, Q. & Wei, Y., 2018. An Inexpensive Apparatus for Classroom Visualization of the Lift on Airplane Wings. The Physics Teacher, 56(9), pp.612–613. https://doi.org/10.1119/1.5080577

Liu, T. et al., 2017. Explicit role of viscosity in generating lift. AIAA Journal, 55(11), 3990-3994. https://doi.org/10.2514/1.J055907

Macchia, S. & Vieyra, R., 2016. A simple wind tunnel to analyse Bernoulli's principle. Physics Education, 52(1), p.013004. https://doi.org/10.1088/1361-6552/52/1/013004

MarkWaller99, 2020. Desktop Windtunnel. YouTube. Available at: https://www.youtube.com/watch?v=Sx5BQjKvElk.

Mclean, J.D., 2012. Understanding aerodynamics: arguing from the real physics, Wiley.

Mclean, D, 2014. Airfoil angle of attack. Wikimedia Commons. Available at: https://commons.wikimedia.org/wiki/File:Airfoil_angle_of_attack.jpg.

Mclean, D., 2018a. Aerodynamic Lift, Part 1: The Science. The Physics Teacher, 56(8), pp.516–520. https://doi.org/10.1119/1.5064558

Mclean, D., 2018b. Aerodynamic Lift, Part 2: A Comprehensive Physical Explanation. The Physics Teacher, 56(8), pp.521–524. https://doi.org/10.1119/1.5064559

MikeRun, 2019. Pitot-tube. Wikimedia Commons. Available at: https://commons.wikimedia.org/wiki/File:Pitot-tube.svg.

Oss, S. et al., 2010. Physics Of Flight At School: The Safe Route. AIP Conference Proceedings. https://doi.org/10.1063/1.3479887

Palmer, B., 2013. Understanding Air France 447, William Palmer, Jr.

Popoola, I., 2017. The U Tube Manometer lg. YouTube. Available at: https://www.youtube.com/watch?v=2P5_J5JEHTQ.

Salas, E.B., Topic: The pilot shortage. Statista. Available at: https://www.statista.com/topics/4324/the-pilot-shortage/#topicHeader__wrapper.

Sheldahl, R. E., & Klimas, P. C., 1981. Aerodynamic Characteristics of Seven Symmetrical Airfoil Sections Through 180-degree Angle of Attack for Use in Aerodynamic Analysis of Vertical Axis Wind Turbines (SAND80-2114). S. N. Laboratories. https://www.osti.gov/servlets/purl/6548367

Thornhill, T., 2017. The most amazing plane facts ever. Daily Mail Online. Available at: https://www.dailymail.co.uk/travel/travel_news/article-4185292/The-amazing-plane-facts-ever.html.

Weltner, K., 1990. Aerodynamic lifting force. The Physics Teacher, 28(2), pp.78–82. https://doi.org/10.1119/1.2342944

Wild, G., 2021. On the Origins and Relevance of the Equal Transit Time Fallacy to Explain Lift. arXiv.org. Available at: https://doi.org/10.48550/arXiv.2110.00690